https://doi.org/10.1016/j.jclepro.2021.126702

Characterising the Resilient Behaviour of Pavement Subgrade with Construction and Demolition Waste under Freeze–Thaw Cycles

Junhui Zhang[1*], Anshun Zhang[2], Chao Huang[3], Huayang Yu[4], Chao Zhou[5]

[1] National Engineering Laboratory of Highway Maintenance Technology, Changsha University of Science & Technology (corresponding author), Changsha, China, Email: zjhseu@csust.edu.cn
[2] National Engineering Laboratory of Highway Maintenance Technology, Changsha University of Science & Technology, Changsha, China, Email: zas@stu.csust.edu.cn
[3] National Engineering Laboratory of Highway Maintenance Technology, Changsha University of Science & Technology, Changsha, China, Email: huangchao@stu.csust.edu.cn
[4] National Engineering Laboratory of Highway Maintenance Technology, Changsha University of Science & Technology, Changsha, China; School of Civil Engineering and Transportation, South China University of Technology, Guangzhou, China, Email: huayangyu@scut.edu.cn
[5] Department of Civil and Environmental Engineering, Hong Kong Polytechnic University, Hung Hom, Hong Kong, Email: c.zhou@polyu.edu.hk

ABSTRACT:

Recycling construction and demolition (C&D) waste as fillers in pavement subgrade is a sustainable paving technology with environmental and economic merits. The performance of pavement subgrade with C&D waste depends on its dynamic resilient modulus. Meanwhile, freeze–thaw cycles are also an important issue for engineering in seasonal frozen regions. However, research on characteristics of the dynamic resilient modulus of C&D waste, especially the properties under freeze–thaw cycles, is limited. To this end, this study aims to reveal the variation law of the dynamic resilient modulus of C&D waste under repeated freeze–thaw cycles and establish a reasonable performance prediction model. This study conducts a series of laboratory tests after various freeze–thaw cycles. Results indicate that the soil–water characteristic curves of C&D waste with different compactness and number of freeze–thaw cycles can be well described by Van Genuchten's model. Moreover, the dynamic resilient modulus enhances with the increase of matric suction, compactness, deviator stress and

minimum bulk stress and exhibits a stress-hardening characteristic. Freeze–thaw cycles attenuate the matric suction and dynamic resilient modulus of C&D waste. Besides, high moisture contents, low stress levels and more freeze–thaw cycles all aggravate the attenuation of the dynamic resilient modulus in certain extent, but the attenuation is not sensitive to the compactness. Finally, this study establishes a high-accuracy prediction model of the dynamic resilient modulus considering the effect of repeated freeze–thaw cycles. This study can supply useful information on the application of C&D waste in pavement subgrade in seasonal frozen regions.

KEYWORDS: Construction and demolition waste; Freeze–thaw cycles; Matric suction; Dynamic resilient modulus; Prediction model

1. INTRODUCTION

The acceleration of the urbanisation process inevitably generates significant construction and demolition (C&D) waste (Wu et al., 2019a). In China, C&D waste continues to accumulate at a rate of approximately 3.5 billion tons every year, but the recycling rate is only 10%. Fig. 1 shows the concentration of C&D waste in all waste and the recycling rate in some countries. The recycling efficiency of C&D waste in China is lower compared with that in developed countries and the efficient use of C&D waste is urgent. Unfortunately, limited domestic engineering projects utilising C&D wastes exist (Zheng et al., 2017), almost all of untreated C&D waste have been piled up in landfills or rural areas, bringing heavy burden to environment and threatening human health (Wu et al., 2019b). The landfill of C&D waste occupies valuable lands, and brings environmental concerns including global warming, soils degradation, and water pollution (Silva et al., 2019). Therefore, exploring an effective and sustainable

development model to recycle C&D waste is crucial.

Recycling C&D waste into construction materials has been a hot research topic for pavement researchers (Yu et al., 2017). Correspondingly, the wide application of asphalt and cement concrete pavement makes it possible to expend vast amount of C&D waste (Leng et al., 2018). In addition to the environmental merits, recycling C&D waste is also an economy-saving approach as the application of C&D waste reduces the material cost in pavement construction (Zhang et al., 2019a). Studies have been conducted to recycle C&D waste as construction materials for pavement surface layers (Yu et al., 2019) and bases or subbases (Saberian et al., 2020). However, given the poor mechanical performance of C&D waste, it can usually only partially replace the materials for pavements upper layers by 20%–50% (Nwakaire et al., 2020). Such reuse efficiency is not quite powerful to consume the tremendous amount of C&D waste in China. Contrastingly, the requirements for pavement subgrade fillers are low. The national highway network planning in China (2013–2030) states that 47,000 km of expressways and 100,000 km of national roads will be built during this period. Concurrently, considering that it typically requires subgrade filling with a depth of 3 m, which indicates that the construction of subgrade needs massive amount of fillers. Thus, recycling C&D waste as alternative fillers to replace natural soils and gravels in pavement subgrade is a promising technology.

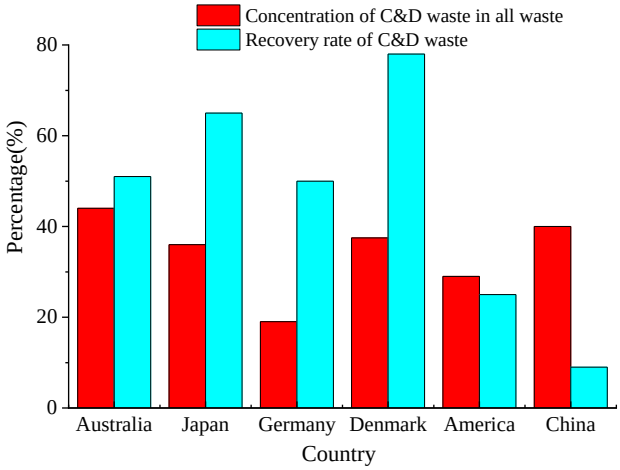

Fig. 1. The concentration of C&D waste in all waste and recovery rate in some countries (Li et al., 2019b)**.**

The dynamic resilient modulus (M_R) is a key engineering parameter for evaluating the stiffness characteristics of subgrade fillers, as it is used in pavement structures design, for example, in the design guide of the American Association of State Highway and Transportation Officials (AASHTO 2002) and the design standard of asphalt pavement in China (JTG D50-2017). Moreover, to allow C&D waste to be widely applied in subgrade construction, it should not only satisfy stiffness requirements, but should also adapt to the complex and changeable climate environment. According to the investigation, the distribution area of seasonal frozen regions diffusely accounts approximately 53.5% and 23% of China's and of the world's total land area, respectively (Zhou et al., 2018). Subgrades located in seasonal frozen regions are exposed to one or more freeze–thaw (FT) cycles every year (Liu et al., 2016). The complicated temperature–load action formed by FT cycles and cyclic traffic loads attenuates the M_R of subgrade fillers more or less, which has been generally approved by researchers (Lu et al., 2018). Nonetheless, limited studies have been undertaken to reveal the characteristics of the M_R of C&D waste as alternative subgrade fillers, especially considering the deterioration caused by FT cycles.

Based on the above analysis, this study aims at providing a comprehensive study to clearly understand the M_R of subgrade C&D waste under FT cycles. Accordingly, this study firstly sets out to review previously published relevant literatures. Thereafter, this study presents experimental results from a series of laboratory tests on C&D waste after FT cycles. Subsequently, this study highlights the influence of various factors on the M_R of C&D waste and an improved prediction model. Finally, this study summarises several major conclusions in the last section.

2. LITERATURE REVIEW

Mechanistic-empirical methods need the M_R value of subgrade fillers as a basic input in order to calculate the stresses and strains in the pavement layers. According to available specifications, the M_R is defined as the ratio of applied deviator stress (σ_d) to resilient deformation (ε_r). Some published studies have been conducted in recent years on the M_R of C&D waste.

Usually, the M_R can be measured in the laboratory by the dynamic triaxial test. Arulrajah et al. (2012) texted the M_R of C&D waste mixed with 10%, 15%, 20%, 25%, 30%, 40%, and 50% crushed brick at 65%–90% of the optimum moisture content (OMC) and the maximum dry density (MDD). The results indicated the concentration level of crushed brick beyond 25%, the M_R values were unsatisfactory on subbases applications. Also, compared with the moisture content, the effect of crushed brick content on the M_R of C&D waste was marginal. For the specimens were compacted to the target state with the OMC and the MDD, Disfani et al. (2014) discussed the influence of crushed brick content on the M_R value. The conclusions emphasized the C&D waste with up to 50% crushed brick and 3% cement were suitable for applications

such as cement-stabilized pavement subbases. Arisha et al. (2016) performed the dynamic triaxial test in accordance with the AASHTO T307 on subbases C&D waste based on the OMC and the MDD, the data showed that the M_R yielded high values and were sensitive to changes in stress states. Arulrajah et al. (2019) studied the effect of the moisture content (70% and 90% of the OMC) and the stress states on the subbases C&D waste at the MDD. The authors uncovered that the influence of moisture content on the M_R is negative. Meanwhile, the increasing of confining pressure and deviator stress enhanced the M_R. In another work, a similar experimental rule between stress states and the M_R was also reported by Perera et al. (2019). Saberian et al. (2020) investigated the use of C&D waste under the OMC and the MDD as the bases or subbases course in pavement construction. They reported the M_R results meet the recommended ranges for bases and subbases. Moreover, the addition of glass increases the M_R value significantly. These published literatures provided valuable findings for understanding the M_R of C&D waste, however it is crucial that laboratory testing conditions should represent those of the field as much as possible. In fact, during the service life of subgrades, the moisture content of subgrade fillers is not constant, but gradually exceeds to the OMC and eventually stabilised (Zhang et al. 2020b). Simultaneously, even a small change in compactness will affect the M_R of subgrade fillers. Hence, the C&D waste specimens were compacted at the dry side of the OMC or the OMC and the MDD cannot fully cover the working conditions that should be considered. In addition, given that the stress states of various layers in the pavement structure are different due to the diffusion and absorption function, the loading sequences for bases or subbases are not suitable for testing the M_R of subgrade C&D waste. As far as the authors are aware, the aforementioned imperfections remain a gap yet in literature.

On the other hand, the measurement on the M_R of C&D waste from the dynamic triaxial test is rather complicated, due to the expensive procedure and time-consuming nature, attempts have been proposed models to predict it by several variables is also advisable. The M_R is commonly expressed as a phenomenological function, Leite et al. (2011) unveiled that the M_R of C&D waste was highly sensitive to the bulk stress and the k-θ model (Seed et al. 1967) presented in Eq. (1) was used to describe their behaviour.

$$M_R = k_1 \left(\frac{\theta}{P_a} \right)^{k_2} \tag{1}$$

where P_a=101.3kPa, which is the atmospheric pressure; θ is the bulk stress, $\theta=\sigma_1+\sigma_2+\sigma_3$, σ_1, σ_2 and σ_3 are the major principal stress, the intermediate principal stress, and the confining pressure, respectively; and k_1 and k_2 are regression coefficients.

Delongui et al. (2018) believed that the resilient response of C&D waste depended on the confining pressure and established a model as exhibited in Eq. (2), and the prediction effect was satisfactory.

$$M_R = k_1 \left(\sigma_3 \right)^{k_2} \tag{2}$$

Since the Eqs. (1) and (2) just reflects the constraint effect, the shearing behaviour of C&D waste are neglected. For this purpose, Mohammadinia et al. (2018) chose the model was suggested by Puppala et al. (2011) to distinguish the effect of constraint and deviator stress, as shown in Eq. (3). Subsequently, a research on C&D waste from Saberian et al. (2019) demonstrated the predicted value obtained by selecting Eq. (3) was close to the measured value.

$$M_R = k_1 P_a \left(\frac{\sigma_3}{P_a} \right)^{k_2} \left(\frac{\sigma_d}{P_a} \right)^{k_3} \tag{3}$$

where σ_d is the deviator stress, $\sigma_d=\sigma_1-\sigma_3$; and k_3 is regression coefficients.

Although some prediction models on the M_R of C&D waste have been shown to be successful, there are other variables such as the matric suction and compactness that influence it. For natural subgrade soils, Zhang et al. (2019b) developed a comprehensive prediction model for the effects of the confinement effect, shearing effect, compactness and moisture variation on the M_R, as shown in Eq. (4). Its form is simple and the universal triaxial testing system is enough to obtain model parameters. Also, this study verified the model through experimental data of different types of soils, the results showed that the model has a higher prediction accuracy. However, the feasibility for subgrade C&D waste remain poorly understood with the complexity of materials conditions, let alone changeable climate environment.

$$M_R = k_1 P_a C^{k_2} \left(\frac{\psi}{P_a} + 1 \right)^{k_3} \left(\frac{\theta_m}{P_a} \right)^{k_4} \left(\frac{\tau_{oct}}{P_a} + 1 \right)^{k_5} \quad (4)$$

where C is the compactness, defined as the ratio of dry density to maximum dry density; ψ is the matric suction, $\psi=u_a-u_w$; u_a is the pore–air pressure, u_w is the pore–water pressure; $\theta_m=\sigma_1+\sigma_2+\sigma_3-\sigma_d$ is the minimum bulk stress; τ_{oct} is the octahedral shear stress, $\tau_{\mathrm{oct}} = \sqrt{(\sigma_1-\sigma_2)^2+(\sigma_1-\sigma_3)^2+(\sigma_2-\sigma_3)^2}/3 = \left(\sqrt{2}/3\right)\sigma_d$; and $k_1 \sim k_5$ are model parameters.

Literature has also illustrated that the performance of subgrades may be attenuated by FT cycles in seasonal frozen regions. For instance, Liu et al. (2016) found that the M_R of silty soils reduced by 26% to 45% after 7–9 FT cycles, and several similar experimental conclusions about the fiber-reinforced soils (Orakoglu et al. 2017), lime improved soils (Bozbey et al. 2018) and loess (Zhou et al. 2018) were reported in other investigator's works. It is anticipated that it should also affect the M_R value of C&D waste. At present, there are very few studies that have

investigated on this point. Li et al. (2019b) measured the resilient modulus value of C&D waste subjected to FT cycles by pressure testing machine after five cycles of loading and unloading. However, since this kind of approach was based on static loading conditions and was an index of strength, whereas the M_R represented stiffness under dynamic loading and was significantly affected by the stress states, which cannot be represented in their testing. Moreover, this method may not completely eliminate the initial plastic deformation of specimens, leading to possible non-negligible errors in the results.

To address the above series of problems, the specific objectives of this study are to measure the matric suction and the M_R of subgrade C&D waste after FT cycles by the filter paper test and the dynamic triaxial test, respectively, and the levels of moisture content and compactness of specimens covered the possible working conditions of subgrade fillers. Then, this study analysed the influence rules of various factors on the M_R of C&D waste. Meanwhile, this study generated a new prediction model taking into account the FT cycles, compactness, matric suction and stress states. The findings of this study made novel contributions to the literature.

3. MATERIALS AND TESTING PROGRAM

3.1 Field project related to this study

This study was conducted during the construction of the Tongzhou–Daxing section of the capital beltway located in Tongzhou District, Beijing. The length of test section is 100 m. The width and average height of the subgrade filled with C&D waste were 40 m and 5.5 m, respectively.

Table 1 summarises the cost comparison of the subgrade construction between the C&D

193 waste and natural soils.

194 **Table 1. The comparison of cost with different fillers.**

Cost (CNY/m^3)	C&D waste	Soils
Land expropriation	5	45
Materials	0	30
Processing	20	0
Transportation	25	20
Construction	15	10
Total	65	105

195 According to Table 1, when the natural soils is 100% replaced by the C&D waste,
196 approximately 0.88 million CNY can be saved in the subgrade construction of the 100m test
197 section. In addition to the environmental merits on waste management, recycling C&D waste
198 is also a cost-reducing approach for pavement subgrade construction.

199 **3.2 Materials**

200 The C&D waste used in this study were identical with the actual subgrade fillers and all
201 were produced by the same manufacturer, as shown in Fig. 2. The other report confirmed that
202 indicators of C&D waste selected for this project meet requirements of the subgrade filling
203 (Zhang et al., 2020a). The basic properties and particle size analysis of C&D waste are listed in
204 Table 2 and Fig. 3, respectively.

205

Fig. 2. The C&D waste used in this study.

Table 2. The basic properties of the used C&D waste.

W_L	W_P	*MDD*	*OMC*	*Organic content*	*Soluble salt*	*CBR*
28.1%	22.5%	1.81g/cm^3	13.2%	1.90%	0.376%	10% ~ 99%

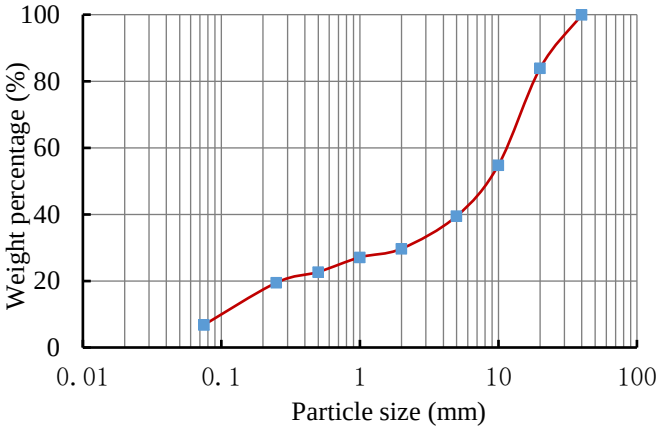

Fig. 3. Gradation curve of the used C&D waste.

3.3 Dynamic triaxial test

3.3.1 Specimens preparation

This study examined the M_R characteristics of C&D waste through dynamic triaxial tests. As mentioned above, the moisture content and compactness significantly affect the M_R. Zhang et al. (2020c) investigated some subgrades in southern China and found that the actual moisture content of these subgrades can reach 116% OMC after nearly 20 years of operation. Another researcher's field monitoring data showed that the moisture content of the subgrade after two years opening to traffic was about 1.1 times of the OMC (Elliott, 1992). Considering the dry and rainless climate in Beijing, this study selected three moisture contents, i.e. OMC, OMC+2% and OMC−2% to cover the range of possible moisture contents of subgrade. To ensure that the compactness research levels set in this study corresponded to the subgrade design standard in

China (JTG D30-2015), this study applied three different levels of compactness, i.e. 96%, 93% and 90%. Given the limited clay content in C&D waste, the specimen is relatively loose at a low compactness. Fig. 4 displays that the specimen at the compactness of failed during the loading process. Therefore, this study considered only two different levels of compactness (93% and 96%).

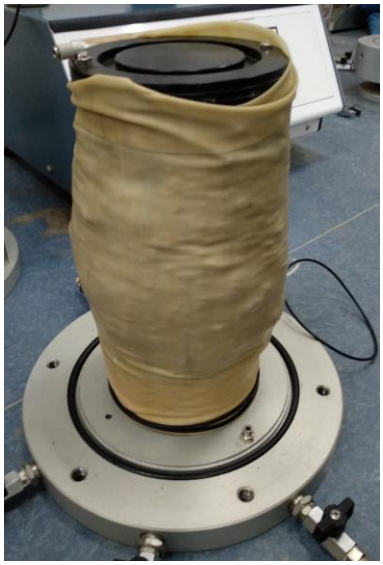

Fig. 4. The failure state of the specimen at the compactness of 90%.

Considering the requirements for the specimen size in dynamic triaxial tests and the range of the particle size of C&D waste, this study prepared cylindrical specimens with a height of 300 mm and a diameter of 150 mm. This study used the self-developed matched forming mould (Fig. 5). This study filled and compacted the five layers of the specimen by a metal bar. Afterwards, this study compacted the specimen to the designed height, which was corresponding to the anticipant compactness. After this study prepared the specimen, the researchers sealed it with plastic wrap to avoid water evaporation. Fig. 6 displays the completed specimens.

Fig. 5. Forming mould.

Fig. 6. Specimens.

236 *3.3.2 Stress sequences and instruments*

237 Given that the main components of C&D waste are crushed concrete, crushed bricks,
238 detritus and so on, the stress–strain characteristics of C&D waste are similar to those of the
239 graded broken stone or coarse-grained soils. For the dynamic triaxial test of the graded broken
240 stone or coarse-grained soils, Andrei et al. (2004) pointed out that the principal stress ratio (r)
241 has a noteworthy effect on the results of the M_R, which was later confirmed by other scholars
242 (Mahinroosta and Poorjafar, 2017). On this basis, this study referred the loading sequences for
243 subgrade coarse-grained soils that considers the principal stress ratio from Luo's doctoral
244 dissertation (Luo, 2007) as described in Table 3.

245 **Table 3. The loading sequences for C&D waste.**

Sequences	Deviator stress (σ_d, kPa)	Confining pressure (σ_3, kPa)	Principal stress ratio ($r=\sigma_1/\sigma_3$)	Number of cycles
0 (Preloading)	60	30	3	1000
1	8	15	1.5	100
2	15	30	1.5	100
3	23	45	1.5	100
4	30	60	1.5	100
5	40	80	1.5	100
6	15	15	2	100
7	30	30	2	100
8	45	45	2	100
9	60	60	2	100
10	80	80	2	100
11	30	15	3	100
12	60	30	3	100

13	90	45	3	100
14	120	60	3	100
15	160	80	3	100

The selected instrument is the dynatriax 100/14 static-dynamic triaxial test system produced by the Italian Controls company (Fig. 7). The cyclic loads with a half-sine load pulse, which had a duration of 0.2 seconds and a rest period of 0.8 seconds, was used in accordance with NCHRP1-28A. Before formal loading, this study eliminated the initial plastic deformation by applying 1,000 preloading cycles to specimens. Then, this study used the test data of the last five cycles to acquire the M_R.

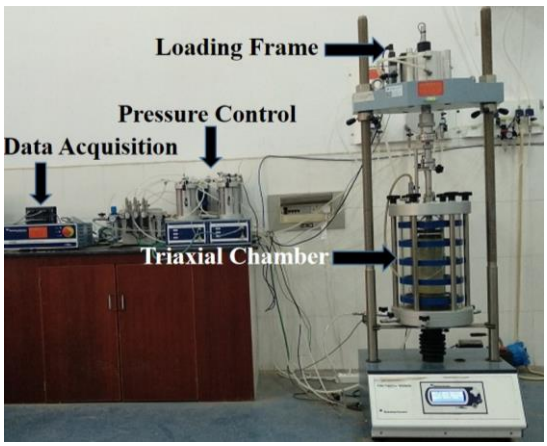

Fig. 7. The dynamic triaxial test system.

3.4 Matric suction measurement

This study selected the filter paper test in ASTM D5298 is widely used to ascertain matric suction of unbound granular aggregates due to its simple operations, accurate results and wide measuring range (Gu et al., 2015). Therefore, this study obtained the soil–water characteristic curve (SWCC) of C&D waste by the filter paper test. Firstly, this study filtered the C&D waste by the No. 4 sieve and formed specimens of 6.18 cm × 2 cm (diameter × height) according to anticipant compactness (93%, 96%) and moisture content (OMC, OMC±2%, OMC±4%, OMC±6%), as shown in Figs. 8(a) and (b). Then, this study placed three pieces of Whatman

NO. 42 type filter papers between the upper and lower specimens and combined the two specimens tightly together with a fresh-keeping film and placed in a sealed jar for 7 d, as shown in Figs. 8(c) and (d). Subsequently, this study measured the equilibrium moisture content of the middle filter paper via an analytical balance. Finally, this study calculated the matric suction of the specimen through the functional relationship between the moisture content and matric suction as shown in Eq. (5) (Leong et al., 2002).

(a) Materials preparation

(b) Specimen molding

(c) Filter paper placed

(d) Sealing and standing

Fig. 8. Main steps of the filter paper test.

$$\lg\psi = \begin{cases} 4.945 - 0.0673w \ (w < 47\%) \\ 2.909 - 0.0229w \ (w \geq 47\%) \end{cases} \tag{5}$$

where ψ is the matric suction; w is the equilibrium moisture content of middle filter paper after

7 days.

3.5 Freeze−thaw cycles setting

Based on the statistical analysis of local climate monitoring in recent years, the lowest temperature in Beijing is −18.7 ℃. Correspondingly, a complete FT process was set to freeze at −20 ℃ for 12 h and thaw at 20 ℃ for 12 h to simulate the possible temperature variations in Beijing. This study covered the specimens fully by plastic wrap and placed in a high–low temperature alternating test box (as shown in Fig. 9), so that the whole FT process was in a closed system without the water replenishment. The number of FT cycles was taken as 0, 1, 3, 6, and 10 in the way of increasing the backward difference to eliminate possible misleading rules. The details for testing the M_R and matric suction of the C&D waste undergoing different FT cycles were consistent with those described in Sections 3.3 and 3.4.

(a) Interior (b) Control interface

Fig. 9. The high–low temperature alternating test box.

4. RESULTS AND DISCUSSION

4.1 Matric suction and soil–water characteristic curve

The M_R of subgrade fillers is significantly affected by the humidity state. Therefore, as a parameter that can better reflect the humidity than the moisture content (Yao et al., 2021), the matric suction of C&D waste should be accurately analysed. Ultimately, this study used the widely applied Van Genuchten's model shown in Eq. (6) (Van Genuchten, 1980) to describe the relationship between the volume moisture content and matric suction of C&D waste undergoing different FT cycles. The coefficients and goodness of Van Genuchten's model and soil–water characteristic curves (SWCC) obtained by this model are shown in Table 4 and Fig. 10, respectively.

$$\frac{\theta_v - \theta_r}{\theta_s - \theta_r} = \left[\frac{1}{1+(a\psi)^n}\right]^m \tag{6}$$

where θ_v is the volume moisture content; θ_s is the saturated volume moisture content, as measured by a saturator; θ_r is the residual volume moisture content; ψ is the matric suction; and *a, n, m* are fitting coefficients.

Table 4. Fitting results of Van Genuchten's model for SWCCs of C&D waste.

Compactness	Cycles	a	n	m	R^2
93%	FT=0	0.289	5.344	0.035	98.69%
	FT=1	0.331	1.556	0.124	98.25%
	FT=3	0.652	6.721	0.028	97.79%
	FT=6	0.919	23.009	0.008	98.35%
	FT=10	1.156	23.008	0.007	97.31%
96%	FT=0	0.248	1.622	0.111	99.02%
	FT=1	0.439	2.408	0.072	99.19%
	FT=3	0.632	24.431	0.008	97.22%
	FT=6	0.807	3.642	0.047	98.53%
	FT=10	0.856	3.347	0.058	98.95%

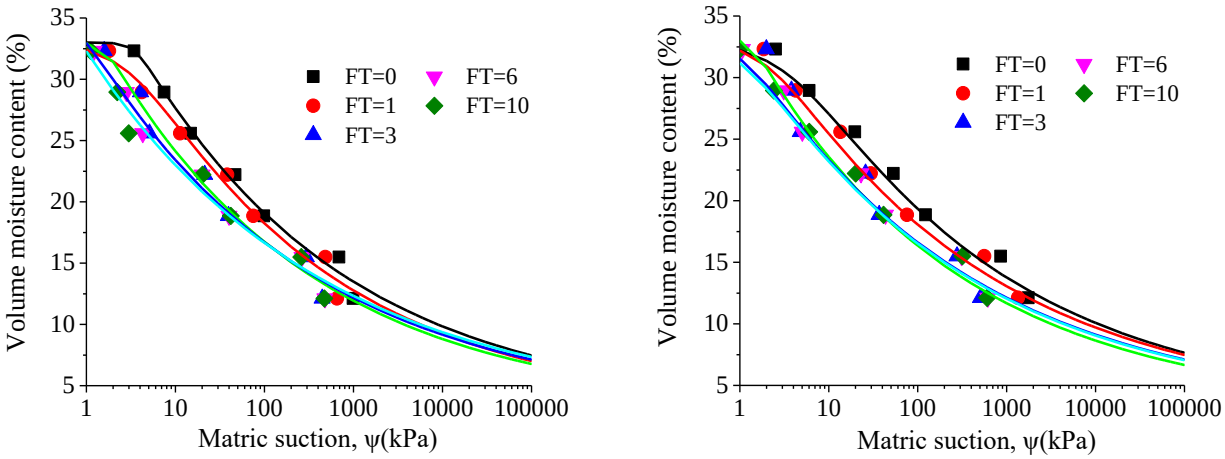

298 **Fig. 10. SWCCs of Van Genuchten's model for C&D waste.**

299 Table 4 exhibits that the SWCCs of specimens with different compactness and suffering
300 various FT cycles have higher model determination coefficient (R^2). As mentioned in Witczak
301 et al. (2002)'s study, a fair fit is defined as $0.4 \leq R^2 \leq 0.69$, a good fit is R^2=0.7–0.89 and an
302 excellent fit is $R^2 \geq 0.9$. Therefore, the relationship between the volume moisture content and
303 matric suction of C&D waste were subjected to FT cycles can be well described by Van
304 Genuchten's model.

305 Fig. 10 shows the measured matric suction and SWCCs of C&D waste under various
306 conditions. The matric suction of C&D waste increases with the increasing compactness at same
307 volume moisture content and FT cycles. In addition, with increasing FT cycles, the matric
308 suction at same compactness and volume moisture content decreases and the SWCC at the same
309 compactness migrates to the bottom left. The matric suction declines significantly after the first
310 FT cycle and stabilises after suffering 6 to 10 FT cycles. The test results can be well explained
311 by the following theory of unsaturated soils mechanics.

312 The matric suction of unsaturated materials was defined as (Fredlund and Xing, 1994):

313 $$\psi = u_a - u_w \quad (7)$$

where u_a and u_w are the pore–air pressure and pore–water pressure respectively.

Simultaneously, the Young–Laplace equation of capillaries can be expressed as (Zhou et al., 2019):

$$u_a - u_w = \frac{2T_s}{R_s} \tag{8}$$

where T_s is the tension on the interfacial between water and air, which is generally considered to be constant; R_s is the curvature radius of the pores between the particles of the material.

Combining Eq. (7) with Eq. (8), a new equation can be obtained as shown in Eq. (9).

$$\psi = \frac{2T_s}{R_s} \tag{9}$$

Based on Eq. (9), the increase of compactness reduces the pores between particles and the curvature radius of the pores so that the matric suction in the same state increases as the compactness increases. Moreover, the water in the pores freezing into ice at a negative temperature and the volume of ice is roughly 9% larger than liquid water during the process of phase transitions (Zhou et al., 2020). The growth of ice crystals makes the particles to be uplifted, but when ice crystals thawing at positive temperatures, the lifted particles cannot be completely restored (Zhou et al., 2018). Thus, a complete process comprising freezing and thawing results in the expansion of pores between particles, increasing of the curvature radius of the pores and the attenuation of matric suction. Furthermore, with increasing FT cycles, the contribution of ice crystals to the lifting of particles decreasing gradually, until the pores between the particles are expanded by repeated FT cycles are large enough to endure the volume growth due to the phase transitions in water, the curvature radius of the pores is no longer enlarged, and the matric suction stops attenuating and remains almost stable.

4.2 Analysis of influencing factors of the dynamic resilient modulus

4.2.1 Influence of deviator stress on the dynamic resilient modulus

Fig. 11 shows the change law of the M_R with deviator stress under different confining pressures, compactness and moisture contents. It can be seen the M_R of C&D waste increases significantly as the deviator stress increases at the same confining pressures, compactness and moisture contents. Taking Fig. 11(a) as an example, the M_R increases by 18.4%, 23.6%, 40.1%, 17.6% and 39.8% when the deviator stress increases from 8 to 30 kPa, 15 to 60 kPa, 23 to 90 kPa, 30 to 120 kPa and 40 to 160 kPa at the 93% compactness and OMC−2%, respectively. Obviously, the C&D waste under cyclic loads shows a clear stress-dependence characteristic.

It is worth noting that C&D waste and graded broken stone exhibit a similar stress-hardening reaction (Gu et al., 2015). One possible explanation is that the increased deviator stress strengthens the unbound C&D waste and produces a smaller elastic deformation under the load. It can be deduced that the subgrade filled with C&D waste should obtain better stability and durability under long-term heavy traffic loads. The octahedral shear stress has the same effect on the M_R as the deviator stress because $\tau_{oct} = \left(\sqrt{2}/3\right)\sigma_d$.

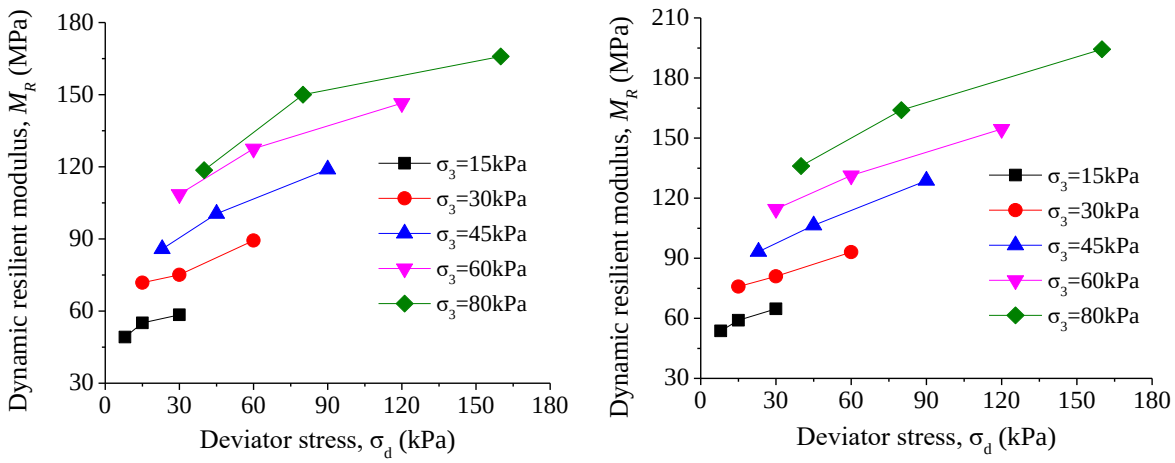

(a) K=93%, OMC-2% (b) K=96%, OMC-2%

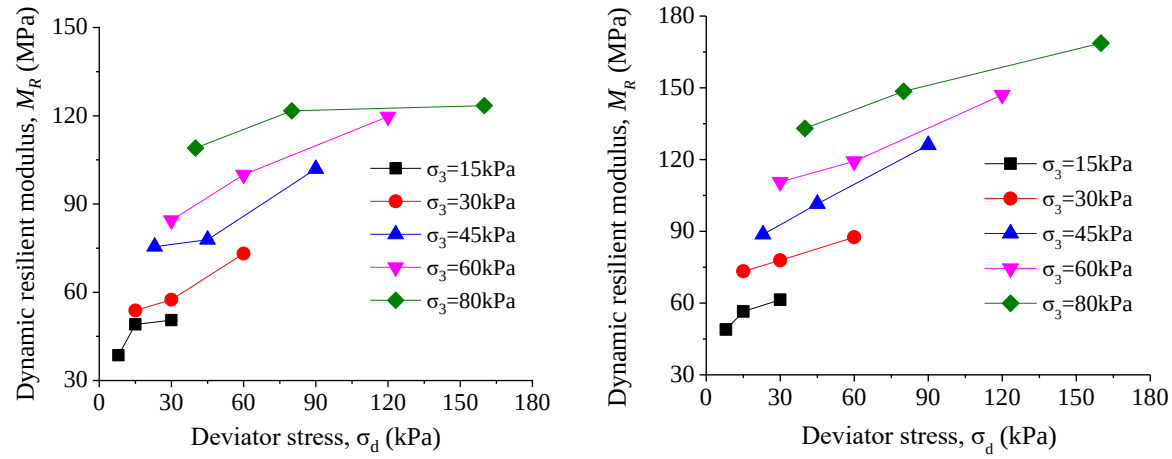

(c) K=93%, OMC (d) K=96%, OMC

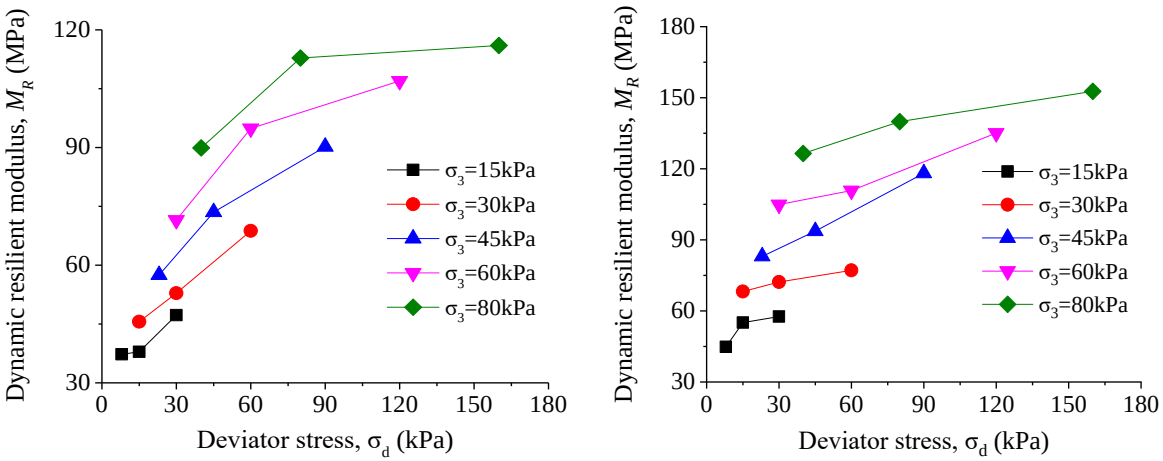

(e) K=93%, OMC+2% (f) K=96%, OMC+2%

Fig. 11. Relationship between the deviator stress, confining pressure and M_R at FT=0.

4.2.2 Influence of minimum bulk stress on the dynamic resilient modulus

Compared with the bulk stress $\theta=\sigma_1+\sigma_2+\sigma_3=3\sigma_3+\sigma_d$, Zhang et al. (2019b) defined a new variable named the minimum bulk stress ($\theta_m=\sigma_1+\sigma_2+\sigma_3-\sigma_d=3\sigma_3$) to separate the shear effect of specimens from the bulk stress, which avoids the bulk stress reflects two contrary effects, namely, hardening effect and softening effect. Thus, the minimum bulk stress can be selected to factually reflect the restriction effect on the M_R. Fig. 12 presents that the M_R increases with the increase of the minimum bulk stress under the given moisture content, compactness and principal stress ratio (σ_1/σ_3). The increase in principal stress ratio helps the M_R increase at various same conditions. For instance, Fig. 12(a) reveals that at 93% compactness and OMC−2%, when the minimum bulk stress is from 45 to 240 kPa, the M_R is increased by 140.8%,

172.7% and 184.5% under the principal stress ratios of 1.5, 2 and 3, respectively. And then, when the principal stress ratio is from 1.5 to 3, the M_R is increased by 18.3%, 25.4%, 38.4%, 35.2% and 39.8% under the value of minimum bulk stresses of 45 kPa, 90 kPa, 135 kPa, 180 kPa and 240 kPa, respectively. This is because for the unbound C&D waste fillers, the increase in the restriction effect results in tight combinations between the particles inside C&D waste and strong resistance to deformation.

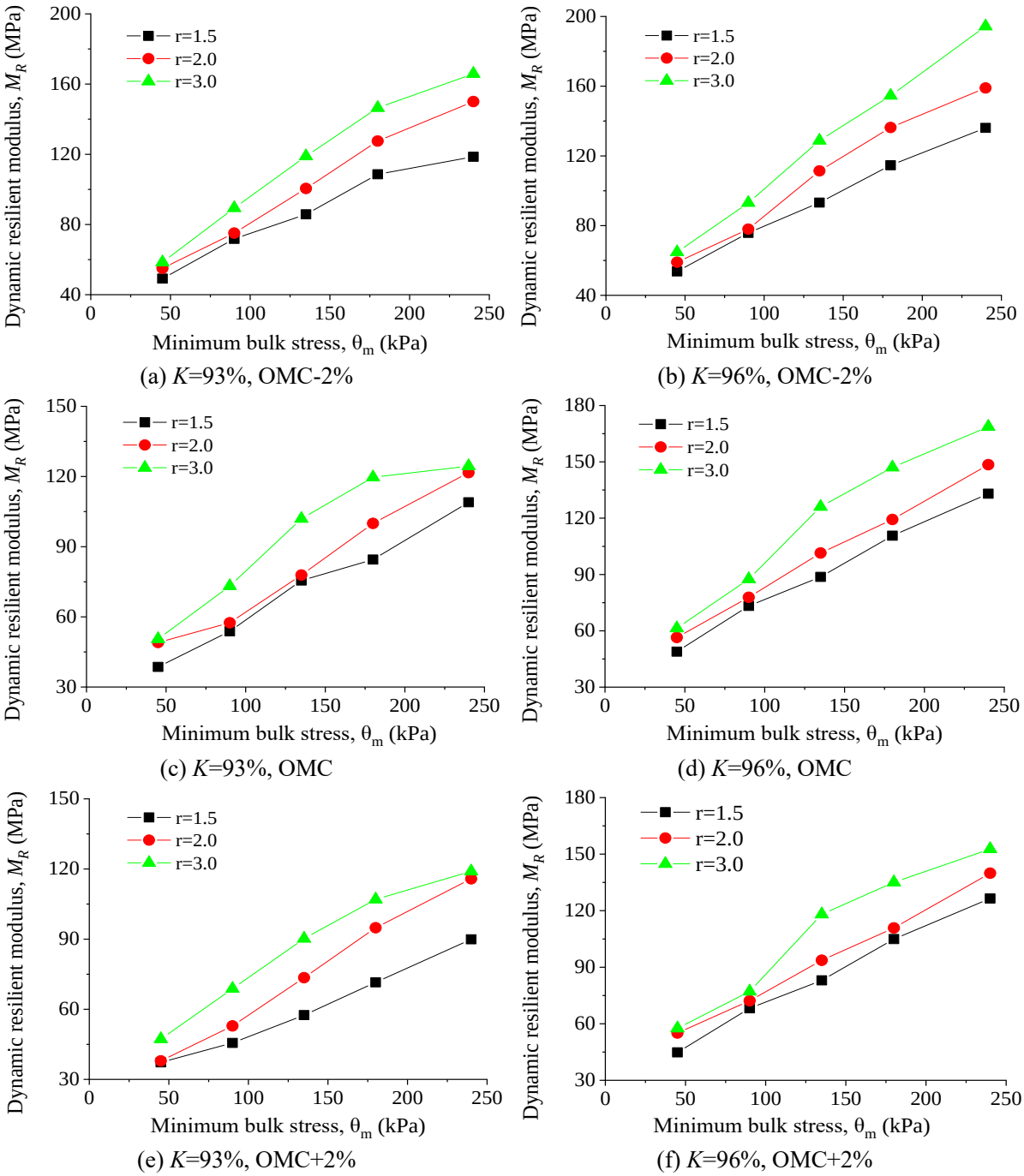

(a) K=93%, OMC-2%

(b) K=96%, OMC-2%

(c) K=93%, OMC

(d) K=96%, OMC

(e) K=93%, OMC+2%

(f) K=96%, OMC+2%

Fig. 12. Relationship between the minimum bulk stress, principal stress ratio and M_R at FT=0.

4.2.3 Influence of compactness on the dynamic resilient modulus

Figs. 11 and 12 present that under the same stress state and moisture content, the greater the compactness, the larger the M_R. For example, comparing Fig. 12 (c) with Fig. 12 (d) unveils that under OMC and the maximum principal stress ratio (r=3), the increase in compactness of 3% enhances the M_R by 19.6%, 19.2%, 23.5%, 22.3% and 38.8% when the minimum bulk stress is 45 kPa, 90 kPa, 135 kPa, 180 kPa and 240 kPa, respectively. Therefore, better compaction of the subgrade filled with C&D waste can contribute to reducing its deformation in the service period.

4.2.4 Influence of matric suction on the dynamic resilient modulus

Fig. 13 shows the relationship between the matric suction and M_R at diverse compactness (93% and 96%). At the same compactness, the M_R increases with increasing matric suction, but it is not a simple linear rise. The positive correlation between the M_R and matric suction is explained as follows. For unsaturated C&D waste specimens, the pores between the particles are filled with moisture and air, and the moisture and air form an interface in every pore. As the matric suction increases, the curvature radius of the moisture–air interface decreases and induces greater contact forces between the particles (Liang et al., 2008). The improved contact force hinders the relative sliding between the particles under load and promotes the specimen to be more robust and stable (Ng and Pang, 2000).

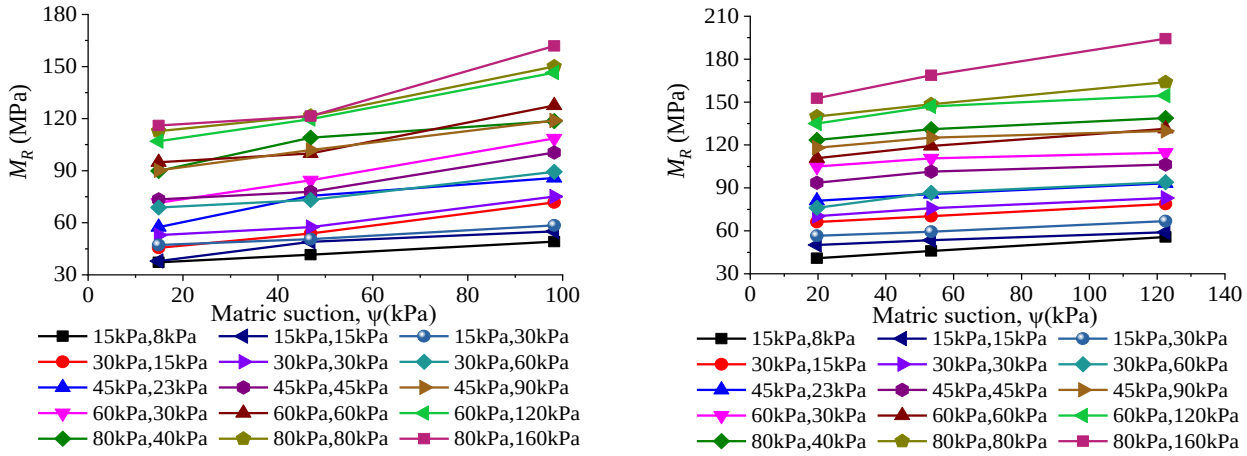

(a) K=93% (b) K=96%

Note: (15kPa, 8kPa) denotes that the confining pressure is 15kPa, and the deviator stress is 8kPa.

Fig. 13. Relationship between the matric suction and M_R at FT=0.

4.2.5 Influence of freeze–thaw cycles on the dynamic resilient modulus

To reveal the weakening of the M_R of C&D waste caused by repeated FT cycles, this study took FT damage factor as an evaluation index, which was defined as:

$$D = \frac{M_{R(0)} - M_{R(i)}}{M_{R(0)}} \tag{10}$$

where D is the damage factor; $M_{R(0)}$ is the M_R without FT cycles; $M_{R(i)}$ is the M_R undergoing the FT cycle with times i, where i=0, 1, 3, 6, 10.

Fig. 14 shows that under the given moisture content, compactness and stress state, the M_R gradually declines until it remains stable after suffering 6 FT cycles, and the first FT cycle has the greatest damage to the M_R. The attenuation range of the M_R is about 15%–42%. This is because repeated alternations of positive and negative temperatures lead to continuous freezing-thawing-freezing of water in the pores. In this process, the volume of water increases and particles are constantly lifted (Zhou et al., 2018), resulting in the increase of pores and the decrease of stiffness. When the expanded pores are large enough to accommodate the growing ice crystals, the internal structure of the specimen is no longer degraded. As for C&D waste,

403 the ice crystal is the most violent to the rise of particles under the action of the first FT and
404 achieve a stable condition must go through nearly 6 cycles. In addition, if the stiffness loss of
405 C&D waste due to repeated FT cycles is ignored, the support of the subgrade to the pavement
406 will be overestimated. Li et al. (2019a) pointed out that 18.7% of attenuation for M_R would lead
407 to the tensile stress at the bottom of asphalt surface layer increases by 10.6%.

408 Fig. 14 also shows that at the same compactness and stress level, the increase of moisture
409 content aggravates the damage of the M_R to a certain extent caused by FT. This is attributed to
410 the fact that in a closed system without water supply, the more water in the specimen, the more
411 ice crystals in the frozen state to expand the spacing between particles, thereby increasing the
412 number and size of pores. Moreover, with the increase of stress level, in most cases, the damage
413 degree of the M_R after repeated FT cycles is universally weakened. It suggests that the specimen
414 presents a harden phenomenon under the higher deviator stress and confining pressure, which
415 may be offsetting a part of the damage after suffering once or more FT cycles. Resultantly, it
416 shows a better ability to maintain stiffness than that under a low-stress state.

417 Ultimately, Fig. 14 reveals that the FT damage factor is not sensitive to the compactness
418 changes under the same moisture content and stress state. By analysing the Eq. (10), when the
419 other conditions are constant, although the M_R corresponding to the 93% compactness is smaller
420 than that under the 96% compactness, there are larger and more pores in the specimen under
421 the 93% compactness than that under the 96% compactness for the free growth of ice crystals.
422 The change in the internal structure of the specimen under the 93% compactness is relatively
423 small which results in a smaller M_R attenuation. This leads to the damage factors corresponding
424 to the two compactness in the same conditions close to each other.

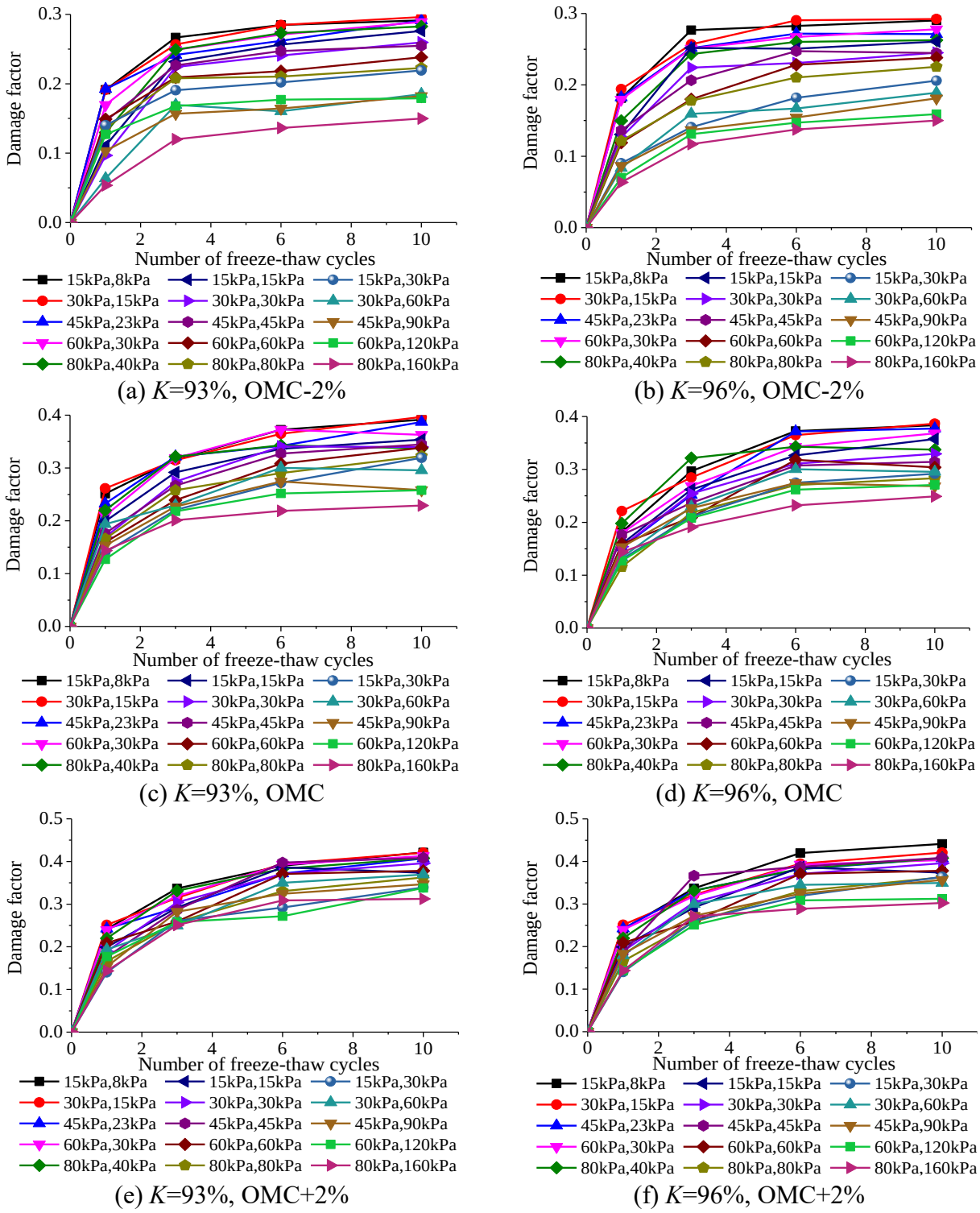

425 **Fig. 14. Damage factors of M_R after FT cycles under different working conditions.**

426 **4.3 Model for predicting the dynamic resilient modulus of construction and demolition**

427 **waste under freeze–thaw cycles**

428 A logical prediction model used to guide relevant engineering applications should fully

include influencing factors and accurately reflect the influence of each factor on the M_R. The number of FT cycles, compactness, humidity and stress state should be considered in the prediction model of the M_R of C&D waste fillers in seasonal frozen areas. It can be seen from Fig. 14 that the attenuation rate of the M_R caused by FT effect gradually decelerates with the increase of cycle number, which is similar to the change rule of the logarithmic function. Therefore, this study adopted a logarithmic form to incorporate the number of FT cycles into Eq. (4), as shown in Eq. (11).

$$M_R = k_1 P_a \left[ln\left(N + e\right) \right]^{k_2} C^{k_3} \left(\frac{\psi}{P_a} + 1 \right)^{k_4} \left(\frac{\theta_m}{P_a} \right)^{k_5} \left(\frac{\tau_{oct}}{P_a} + 1 \right)^{k_6} \tag{11}$$

where C is the compactness; N is the number of FT cycles; $k_1 \sim k_6$ are the model parameters, and other symbols have the same meaning as above.

For Eq. (11), this prediction model has fully considered the influencing factors and is easy to be understood. Moreover, model parameters are easily acquired and have explicit meanings. k_1 is the adjustment coefficient that is proportional to the M_R, which can be determined to be a positive number because the M_R cannot be negative. k_2 is the adjustment coefficient of the number of FT cycles, which is helpful to optimise the prediction effect of the prediction model. Meanwhile, k_2 as an exponent must be a negative number, given that with the increase of the number of FT cycles, the M_R decreases. As a parameter embodying the influence of compactness on the M_R, k_3 is a positive number due to the higher the compactness, the larger the M_R. k_4 must be a positive number because the matric suction has a positive effect on the M_R. Based on the hardening effect of the minimum bulk stress and deviator stress (octahedral shear stress) on the C&D waste specimens, it can be concluded that $k_5 > 0$ and $k_6 > 0$.

This study fitted the test results of all the specimens to the prediction model shown in Eq.

(11). Table 5 summarises the obtained coefficients and accuracy of the model. The fit should be considered as an excellent one because the accuracy (R^2) of the model as shown in Eq. (11) is greater than 0.9. At present, few studies have simultaneously analysed change rules of the M_R under repeated FT cycles, matric suction, compactness and stress state. Therefore, acquiring corresponding data in existing literatures to directly verify Eq. (11) is difficult. From another point of view, for the special case (N=0) that does not undergo the FT process, $[ln(N+e)]^{k2}$ is always equal to 1, and then Eq. (11) is completely transformed to Eq. (4). Whilst Eq. (4) has been proved to have a wide range of applications and high prediction accuracy (Zhang et al., 2019b). Further, combining the attenuation trend of the M_R with the number of FT cycles shown in Fig. 14 and the excellent fit shown in Table 5, it can be concluded that the M_R of subgrade C&D waste suffering repeated FT cycles can be predicted by the new model established in this study.

Table 5. The coefficients and accuracy of the model in this study.

k_1	k_2	k_3	k_4	k_5	k_6	R^2	Correlation
0.651	-0.196	3.547	0.446	0.441	1.019	0.94	Excellent

It is worth emphasizing that the model presented in this study is not only valuable to better design the stable and durable regenerated pavement subgrade in seasonal frozen regions, but also helpful to further improve C&D waste recycling performance, and dramatically mitigate land use and correlative pollution in China. Fundamentally, the model established in this study for predicting the M_R of C&D waste under FT cycles is universally applicable. Concretely, when this model is applied to other C&D waste, re-fitting the model parameters based on the test data is necessary. This approach proposed in this study could provide significant references on the similar engineering applications in seasonal frozen regions, such as Russia, Japan, Britain, the Netherlands and so on.

5. CONCLUSIONS

This study tried to gain a better understanding for the M_R of subgrade C&D waste under FT cycles so that construct the high-efficiency resource reuse technology. For this purpose, the feasibility of recycling C&D waste as pavement subgrade fillers in Northern China was evaluated through the basic performance, the filter paper and dynamic triaxial tests after different FT cycles. On the basis of the laboratory test results, the following key findings of this study can be synthetized here:

(1) Under the same conditions, the matric suction of C&D waste increases with the increase of compactness. Meanwhile, the matric suction is attenuated by the continuous FT action until the change of matric suction is not obvious after 6 to 10 cycles. The SWCCs of C&D waste under different compactness and the number of FT cycle can be well described by the Van Genuchten's model.

(2) The M_R of C&D waste is positively correlated with the deviator stress, minimum bulk stress, compactness and matric suction. Moreover, C&D waste shows an obvious stress dependence characteristic, and the stress-hardening reaction is the same as that of graded broken stone.

(3) Low moisture content and high stress level decelerates the damage of M_R caused by repeated FT cycles. With increasing FT cycles, the damage degree of M_R gradually increases but the rate reduces. For subgrade filled with the C&D waste in seasonal frozen regions, the value of M_R after 6 FT cycles can be used as designing parameters of the pavement structure.

(4) This study established a new model, including the number of FT cycles, matric suction, minimum bulk stress, octahedral shear stress and compactness. The results showed that the

proposed model has a high fitting degree and can accurately predict the M_R of C&D waste in seasonal frozen regions.

ACKONWLEDGEMENTS

This work was supported by the National Natural Science Foundation of China (51911530215, 51878078, 52025085, 51927814), Training Program for High-level Technical Personnel in Transportation Industry (2018-025), the design theory, method and demonstration of durability asphalt pavement based on heavy-duty traffic conditions in Shanghai area (CTKY-PTRC-2018-003), and the Open Fund of National Engineering Laboratory of Highway Maintenance Technology (kfj190106, Changsha University of Science & Technology). The authors thank the editor, the associate editor, and all anonymous reviewers for their insightful and constructive comments.

REFERENCES

Andrei, D., Witczak, M.W., Schwartz, C.W., Uzan, J., 2004. Harmonized resilient modulus test method for unbound pavement materials. Transport. Res. Rec. 1874(1), 29-37. http://doi.org/10.3141/1874-04

Arisha, A., Gabr, A., Badawy, S., Shwally, S., 2016. Using blends of construction & demolition waste materials and recycled clay masonry brick in pavement. Pro. Eng. 143, 1317-1324. https://doi.org/10.1016/j.proeng.2016.06.148

Arulrajah, A., Mohammadinia, A., Maghool, F., Horpibulsuk, S., 2019. Tire derived aggregates as a supplementary material with recycled demolition concrete for pavement applications. J. Clean. Prod. 230, 129-136. https://doi.org/10.1016/j.jclepro.2019.05.084

516 Arulrajah, A., Piratheepan, J., Bo, M.W., Sivakugan, N., 2012. Geotechnical characteristics of
517 recycled crushed brick blends for pavement sub-base applications. Can. Geotech. J.
518 49(7), 796-811. https://doi.org/10.1139/t2012-041
519 Bozbey, I., Kelesoglu, M.K., Demir, B., Komut, M., Comez, S., Ozturk, T., Mert, A., Ocal, K.,
520 Oztoprak, S., 2018. Effects of soil pulverization level on resilient modulus and freeze
521 and thaw resistance of a lime stabilized clay. Cold Reg. Sci. Technol. 151, 323-334.
522 https://doi.org/10.1016/j.coldregions.2018.03.023
523 Delongui, L., Matuella, M., Núñez, W., Fedrigo, W., Filho, L., Ceratti, J., 2018. Construction
524 and demolition waste parameters for rational pavement design. Constr. Build. Mater.
525 168, 105-112. https://doi.org/10.1016/j.conbuildmat.2018.02.086
526 Disfani, M., Arulrajah, A., Haghighi, H., Mohammadinia, A., Horpibulsuk, S., 2014. Flexural
527 beam fatigue strength evaluation of crushed brick as a supplementary material in cement
528 stabilized recycled concrete aggregates. Constr. Build. Mater. 68, 667-676.
529 https://doi.org/10.1016/j.conbuildmat.2014.07.007
530 Elliott, R.P., 1992. Selection of subgrade modulus for AASHTO flexible pavement design.
531 Transport. Res. Rec. 1354, 39-44.
532 http://onlinepubs.trb.org/Onlinepubs/trr/1992/1354/1354-003.pdf
533 Fredlund, D.G., Xing, A., 1994. Equations for the soil-water characteristic curve. Can.
534 Geotech. J. 31(4), 521-532. https://doi.org/10.1139/t94-061
535 Gu, F., Sahin, H., Luo, X., Luo, R., Lytton, R.L., 2015. Estimation of resilient modulus of
536 unbound aggregates using performance-related base course properties. J. Mater. Civ.
537 Eng. 27(6), 04014188. https://doi.org/10.1061/(asce)mt.1943-5533.0001147
538 Leite, F., Motta, R., Vasconcelos, K., Bernucci, L., 2011. Laboratory evaluation of recycled

539 construction and demolition waste for pavements. Constr. Build. Mater. 25, 2972-2979.
540 https://doi.org/10.1016/j.conbuildmat.2010.11.105
541 Leng, Z., Padhan, R.K., Sreeram, A., 2018. Production of a sustainable paving material
542 through chemical recycling of waste PET into crumb rubber modified asphalt. J. Clean.
543 Prod. 180, 682-688. https://doi.org/10.1016/j.jclepro.2018.01.171
544 Leong, E.C., He, L., Rahardjo, H., 2002. Factors affecting the filter paper method for total and
545 matric suction measurements. Geotech. Test. J. 25(3), 322-333.
546 https://doi.org/10.1520/GTJ11094J
547 Li, J., Zheng, J., Yao, Y., Zhang, J., Peng, J., 2019a. Numerical method of flexible pavement
548 considering moisture and stress sensitivity of subgrade soils. Adv. Civ. Eng. 2019,
549 7091210. https://doi.org/10.1155/2019/7091210
550 Li, Z., Liu, L., Yan, S., Zhang, M., Xia, J., Xie, Y., 2019b. Effect of freeze-thaw cycles on
551 mechanical and porosity properties of recycled construction waste mixtures. Constr.
552 Build. Mater. 210, 347-363. https://doi.org/10.1016/j.conbuildmat.2019.03.184
553 Liang, R.Y., Rabab'ah, S., Khasawneh, M., 2008. Predicting moisture-dependent resilient
554 modulus of cohesive soils using soil suction concept. J. Transport. Eng. 134(1), 34-40.
555 https://doi.org/10.1061/(ASCE)0733-947X(2008)134:1(34)
556 Liu, J., Chang, D., Yu, Q., 2016. Influence of freeze-thaw cycles on mechanical properties of
557 a silty sand. Eng. Geol. 210, 23-32. https://doi.org/10.1016/j.enggeo.2016.05.019
558 Lu, Z., Xian, S., Yao, H., Fang, R., She, J., 2018. Influence of freeze-thaw cycles in the
559 presence of a supplementary water supply on mechanical properties of compacted soil.
560 Cold Reg. Sci. Technol. 157, 42-52. https://doi.org/10.1016/j.coldregions.2018.09.009
561 Luo, Z., 2007. Study on dynamic resilient modulus of subgrade and granular layer. Ph.D.

562 thesis, Tongji University, Shanghai, China. (In Chinese)
563 Mahinroosta, R., Poorjafar, A., 2017. Effect of stress state and particle-size distribution on the
564 stress reduction of sandy soils during saturation. Constr. Build. Mater. 150, 1-13.
565 https://doi.org/10.1016/j.conbuildmat.2017.05.177
566 Mohammadinia, A., Arulrajah, A., D'Amico, A., Horpibulsuk, S., 2018. Alkali-activation of
567 fly ash and cement kiln dust mixtures for stabilization of demolition aggregates. Constr.
568 Build. Mater. 186, 71-78. https://doi.org/10.1016/j.conbuildmat.2018.07.103
569 Ng, C.W.W., Pang, Y., 2000. Experimental investigations of the soil-water characteristics of a
570 volcanic soil. Can. Geotech. J. 37(6), 1252-1264. https://doi.org/10.1139/cgj-37-6-1252
571 Nwakaire, C. M., Yap, S. P., Onn, C. C., Yuen, C. W., Ibrahim, H. A., 2020. Utilisation of
572 recycled concrete aggregates for sustainable highway pavement applications; a review.
573 Constr. Build. Mater. 235, 117444. https://doi.org/10.1016/j.conbuildmat.2019.117444
574 Orakoglu, M.E., Liu, J., Niu, F., 2017. Dynamic behavior of fiber-reinforced soil under
575 freeze-thaw cycles. Soil Dyn. Earthq. Eng. 101, 269-284.
576 https://doi.org/10.1016/j.soildyn.2017.07.022
577 Perera, S., Arulrajah, A., Wong, Y., Horpibulsuk, S., Maghool, F., 2019. Utilizing recycled
578 PET blends with demolition wastes as construction materials. Constr. Build. Mater. 221,
579 200-209. https://doi.org/10.1016/j.conbuildmat.2019.06.047
580 Puppala, A., Hoyos, L., Potturi, A., 2011. Resilient Moduli Response of Moderately Cement-
581 Treated Reclaimed Asphalt Pavement Aggregates. J. Mater. Civ. Eng. 23(7), 990-998.
582 https://doi.org/10.1061/(asce)mt.1943-5533.0000268
583 Saberian, M., Li, J., Boroujeni, M., Law, D., Li, C., 2020. Application of demolition wastes
584 mixed with crushed glass and crumb rubber in pavement base/subbase. Resour. Conserv.

585 Recy. 156, 104722. https://doi.org/10.1016/j.resconrec.2020.104722
586 Saberian, M., Li, J., Nguyen, B., Setunge, S., 2019. Estimating the resilient modulus of
587 crushed recycled pavement materials containing crumb rubber using the Clegg impact
588 value. Resour. Conserv. Recy. 141, 301-307.
589 https://doi.org/10.1016/j.resconrec.2018.10.042
590 Seed, H., Mitry, F., Monosmith, C., Chan, C., 1967. Prediction of pavement deflection from
591 laboratory repeated load tests, NCHRP report 35. Transport. Res. Board. Washington
592 DC, United States. https://trid.trb.org/view.aspx?id=104508
593 Silva, R.V., de Brito, J., Dhir, R.K., 2019. Use of recycled aggregates arising from
594 construction and demolition waste in new construction applications. J. Clean. Prod.
595 236,117629. https://doi.org/10.1016/j.jclepro.2019.117629
596 Van Genuchten, M.T., 1980. A closed-form equation for predicting the hydraulic conductivity
597 of unsaturated soils. Soil Sci. Soc. Am. J. 44(5), 892-898.
598 http://doi.org/10.2136/sssaj1980.03615995004400050002x
599 Witczak, M., Pellinen, T., El-Basyouny, M., 2002. Pursuit of the simple performance test for
600 asphalt concrete fracture/cracking. J. Assoc. Asph. Paving Technol. 71, 767-778.
601 https://trid.trb.org/view/698762
602 Wu, H., Zuo, J., Yuan, H., Zillante, G., Wang, J., 2019a. A review of performance assessment
603 methods for construction and demolition waste management. Resour. Conserv. Recy. 150,
604 104407. https://doi.org/10.1016/j.resconrec.2019.104407
605 Wu, H., Zuo, J., Zillante, G., Wang, J., Yuan, H., 2019b. Status quo and future directions of
606 construction and demolition waste research: A critical review. J. Clean. Prod. 240, 118163.
607 https://doi.org/10.1016/j.jclepro.2019.118163

608 Yao, Y., Ni, J., Li, J., 2021. Stress-dependent water retention of granite residual soil and its
609 implications for ground settlement. Comput. Geotech. 129, 103835.
610 https://doi.org/10.1016/j.compgeo.2020.103835
611 Yu, H., Leng, Z., Zhou, Z., Shih, K., Xiao, F., Gao, Z., 2017. Optimization of preparation
612 procedure of liquid warm mix additive modified asphalt rubber. J. Clean. Prod. 141, 336-
613 345. https://doi.org/10.1016/j.jclepro.2016.09.043
614 Yu, H., Zhu, Z., Zhang, Z., Yu, J., Oeser, M., Wang, D., 2019. Recycling waste packaging tape
615 into bituminous mixtures towards enhanced mechanical properties and environmental
616 benefits. J. Clean. Prod. 229, 22-31. https://doi.org/10.1016/j.jclepro.2019.04.409
617 Zhang, H., Li, H., Abdelhady, A., Xie, N., Li, W., Liu, J., Liang, X., Yang, B., 2019a. Fine solid
618 wastes as a resource conserving filler and their influence on the performance of asphalt
619 materials. J. Clean. Prod. 252, 119929. https://doi.org/10.1016/j.jclepro.2019.119929
620 Zhang, J., Ding, L., Li, F., Peng, J., 2020a. Recycled aggregates from construction and
621 demolition wastes as alternative filling materials for highway subgrades in China.
622 J. Clean. Prod. 255, 120223. https://doi.org/10.1016/j.jclepro.2020.120223
623 Zhang, J., Li, F., Zeng, L., Peng, J., Li, J., 2020b. Numerical simulation of the moisture
624 migration of unsaturated clay embankments in southern China considering stress state. B.
625 Eng. Geol. Environ. https://doi.org/10.1007/s10064-020-01916-6
626 Zhang, J., Peng, J., Liu, W., Lu, W., 2019b. Predicting resilient modulus of fine-grained
627 subgrade soils considering relative compaction and matric suction. Road Mater.
628 Pavement Des. https://doi.org/10.1080/14680629.2019.1651756
629 Zhang, J., Peng, J., Zhang, A., Li, J., 2020c. Prediction of permanent deformation for
630 subgrade soils under traffic loading in Southern China. Int. J. Pavement Eng.

https://doi.org/10.1080/10298436.2020.1765244

Zheng, L., Wu, H., Zhang, H., Duan, H., Wang, J., Jiang, W., Dong, B., Liu, G., Zuo, J., Song, Q., 2017. Characterizing the generation and flows of construction and demolition waste in China. Constr. Build. Mater. 136, 405-413. http://doi.org/10.1016/j.conbuildmat.2017.01.055

Zhou, J., Wei, C., 2020. Ice lens induced interfacial hydraulic resistance in frost heave. Cold Reg. Sci. Technol. 171, 102964. https://doi.org/10.1016/j.coldregions.2019.102964

Zhou, Y., Zhou, J., Shi, X., Zhou, G., 2019. Practical models describing hysteresis behavior of unfrozen water in frozen soil based on similarity analysis. Cold Reg. Sci. Technol. 157, 215-223. https://doi.org/10.1016/j.coldregions.2018.11.002

Zhou, Z., Ma, W., Zhang, S., Mu, Y., Li, G., 2018. Effect of freeze-thaw cycles in mechanical behaviors of frozen loess. Cold Reg. Sci. Technol. 146, 9-18. https://doi.org/10.1016/j.coldregions.2017.11.011